Detection of photoinduced electronic, thermal, and acoustic dynamics of gold film using a transient reflecting grating method under three types of surface plasmon resonance conditions

Kenji Katayama and Tsuguo Sawada
The School of Engineering, The University of Tokyo, 7-3-1 Hongo Bunkyo-ku, Tokyo 113-8656, Japan

Qing Shen
Graduate School of Electro-Communications, The University of Electro-Communications, 1-5-1 Chofugaoka, Chofu-shi, Tokyo 182-0021, Japan

Akira Harata
Graduate School of Engineering Sciences, Kyushu University, 6-1 Kasugakoen, Kasuga-shi, Fukuoka 816-8580, Japan
(Received 6 April 1998)

Mechanisms of unusual signal enhancement observed for transient reflecting grating (TRG) experiments are investigated under three types of surface plasmon resonance (SPR) conditions, where two pump beams only, a probe beam only, or two pump beams and a probe beam, excite surface plasmon. A gold thin film deposited on a glass prism is measured in the Kretschmann configuration with a temporal resolution of tens of picoseconds. The signal under each SPR condition exhibits different characteristic features in signal intensity and transient behavior unlike the usual non-SPR TRG experiments. Under SPR with pump beams, high conversion efficiency from light to heat allows detection of a TRG signal 11 times larger in magnitude and much lower in background level than under a non-SPR with them. Under SPR with the probe beam, diffraction caused by heat-induced spatial modulation as described by complex reflection Fresnel coefficients is theoretically proved to enhance the TRG signal and to change transient behavior, which provides a way to get selective observation of heat diffusion near the surface. When both pump and probe beams excite surface plasmons, an additional signal is observed, almost at the same time as the optical pulse, having 100 times larger intensity than the other signals, which is due to electrons excited at the gold surface. [S0163-1829(98)02337-6]

I. INTRODUCTION

Surface plasmon (SP) is an optically excited collective motion of electrons oscillating under the influence of positive lattice ions. It has been drawing attention in various fields because it is related to many physically important effects such as surface enhanced Raman scattering (SERS) (Ref. 1) and enhancement of second harmonic generation (SHG),[2] and because it can be well applied to chemical and biochemical sensors[3,4] using an extremely sensitive feature to a slight surface property change. It is possible to convert almost all light energy into SP if the light is incident under a surface plasmon resonance (SPR) condition. The strong electric field generated at the surface or interface is the dominant source of enhancement in SERS and SHG and its interaction with molecules on the surface as well as surface roughness provides the operating principle of the sensors. After the interaction, almost all SP energy is converted into heat through a nonradiative relaxation within a few hundred femtoseconds.[5–7] During the last few decades, many researchers have made numerous studies about SP itself and its applications.[8–12]

If we consider SP-generated heat, it seems a photothermal measurement at a metal surface or a metal/liquid interface can be made by using a transient reflecting grating (TRG) method. In a TRG technique, a transient grating is momentarily generated by an interference pattern of two coherent pump beams crossed at a sample surface or interface and the generated transient grating is detected using the reflecting diffraction of a probe beam. The method has been applied to investigate metal and semiconductor surfaces, multilayer films of nanometer thickness and electrochemical interfaces.[13–15] It has provided information about photoexcited carrier dynamics and heat diffusion in a nanometer scale near interfaces. We have also used the TRG method to generate and detect the surface acoustic wave (SAW) of over GHz frequency that is applicable to determination of the elastic property of the surface.[16–18]

In our previous paper,[19] we reported on TRG signal enhancement under an SPR condition for the Kretschmann configuration. Under SPR with the pump beams, we observed a signal intensity 11 times larger than that under a nonresonant condition, which we attributed to high conversion efficiency from light to heat. Under SPR with the probe beam, we also observed unexpected signal enhancement accompanied by a transient wave form change. We qualitatively explained the dominating factor of the enhancement as a reflectivity modulation term, caused by temperature rise, although that term has been neglected in prior research.

In this article, we describe in detail TRG signal enhancement under three types of SPR conditions, namely, SPR for two pump beams only, SPR for a probe beam only, and SPR for two pump beams and a probe beam. For the last case, we found another enhanced signal with 100 times larger inten-

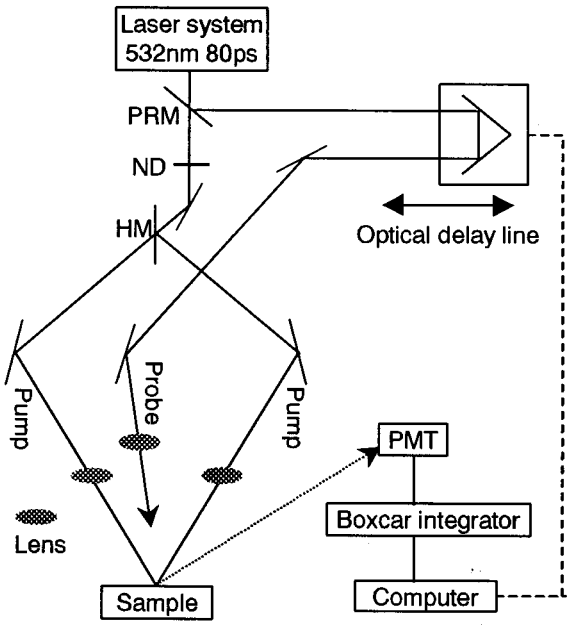

FIG. 1. Experimental arrangement of the transient reflecting grating method. (HM) half mirror, (ND) neutral density filter, (PRM) partial reflective mirror, (PMT) photomultiplier tube, ($\lambda/2$) half wave plate. The other optical elements are prisms and mirrors.

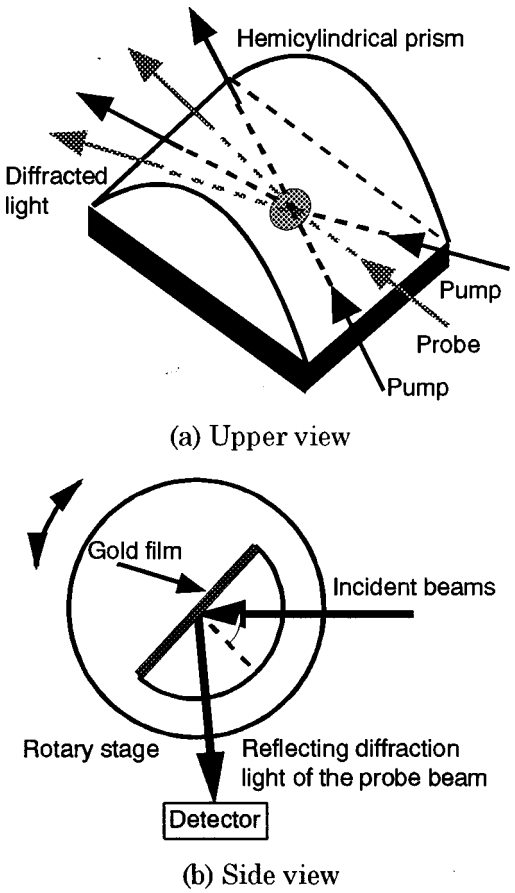

FIG. 2. Schematic illustration of the arrangement of the sample and the laser beams. The two pump beams overlap and form an interference fringe pattern on the gold film/prism interface. The generated transient grating is detected by the reflecting diffraction of the probe beam. The incident angles may be varied using the rotary stage.

sity than under a non-SPR condition, almost at the same time as the optical pulse, which was observed independently from a so-called self-diffraction caused by coherent interaction between one of the pump beams and the probe beam. The next section describes the SPR-TRG experiment. In Sec. III, mechanisms of signal enhancement are theoretically treated on the basis of a thermally induced change in reflection Fresnel coefficients. The results of the theoretical calculation and the experiment are compared and discussed in Sec. IV. Section V summarizes the present work.

II. EXPERIMENT

The experimental arrangement is shown in Fig. 1. A mode-locked *Q*-switched Nd:YAG laser (Quantronix, model 416) was used as the light source. A single pulse was selected from a mode-locked pulse train and was frequency doubled to generate a polarized visible light pulse (wavelength, 532 nm with a repetition rate of 1.03 kHz and pulse width of 84 ps in full width at half maximum). A portion of the light pulse was reflected by a partial reflective mirror to generate a probe pulse. The remainder was halved to generate two pump pulses of the same polarization plane before they were crossed again, coincident in time, to form an interference pattern. Each of the pump pulses was less than 100 nJ/pulse in its time-averaged intensity at the sample and 60 μm in diameter. The arrangement around the sample is enlarged in Fig. 2. The sample was a 36 nm gold film vapor deposited on the surface of a hemicylindrical glass prism made of fused silica of refractive index 1.460 at 532 nm. The prism was loaded on a rotary stage to allow the incident angle of the laser beams to be changed. Angular resolution was better than 1°. Two pump pulses and one probe pulse were incident from the prism side to the gold film, the same as in the Kretschmann configuration, which is often used in attenuated total reflection measurements. These three beams were arranged within the same plane so that the incident angle of the pump beams with respect to the gold film was slightly different from that of the probe beam. The incident angle of the pump beams was 1.3% larger than that of the probe beam when the probe beam bisected the pump beams and the crossing angle of the pump beams was 18.3° in this experimental alignment. This difference was negligible at the present experimental accuracy.

The interference pattern by pump pulses was projected at the prism/gold interface to form the TRG. Grating spacing was controlled by the crossing angle of the pump pulses and was 1.67 μm in this experiment. The probe pulse was incident at the center of the interference fringes after passing through a computer controlled optical delay line. The probe beam was 40 μm in diameter and less than 10 nJ/pulse in intensity. Polarization of the pump and probe beams could be adjusted as *p* polarized or *s* polarized with respect to the metal surface. This was done using two half wave plates. Diffracted light intensity of the probe beam was monitored with a photomultiplier tube (PMT) connected to a flexible light guide, whose entrance was placed at one of the first-

order reflecting diffraction spots. A polarization plate is usually placed before the light guide for TRG measurements in order to reduce the scattered light of the pump beams. However, this time it was removed in order to examine the absolute signal intensity in measurements of various polarizations of pump and probe beams. The output signal from the PMT was gated and averaged over one millisecond with a boxcar integrator (Ortec, 9415, 9425) before analog-to-digital transformation for the computer. A TRG response was obtained on the computer by recording the signal intensity as a function of the delay time of the probe pulse with respect to the pump pulses. The maximum time window of the observation was limited to 13.3 ns by the optical delay line length of 4 m.

For a metal film on a dielectric substrate, TRG is generally formed as surface corrugation caused by spatial modulation of temperature (thermal grating) and a counterpropagating SAW (acoustic grating) having the same wavelength as the optical fringe. Heat generation due to light absorption and nonradiative relaxation followed by thermal expansion generates the thermal grating and the acoustic grating. We observed incident angle dependence of TRG responses under three types of polarization conditions of two pump beams and a probe beam: *p*-polarized pump and *s*-polarized probe; *s*-polarized pump and *p*-polarized probe; and *p*-polarized pump and *p*-polarized probe. A part of the results are shown in Figs. 4, 6, 8, and 9 for discussion in Sec. IV. For comparison of the relative TRG signal intensity, peak height was measured from a baseline, which is the signal level before pump pulses irradiate the sample (delay time <0). Although gains in the detection electronics were not changed during each measurement of the angle dependence, positional rearrangement of the light guide entrance during the angle change, as well as long term laser stability could influence the signal intensity. We estimated such an error was less than 10%.

III. THEORY

A. TRG signal intensity

From simple considerations, the TRG signal amplitude S_{TRG} is proportional to $I_P {P_E}^2 R_P (1-R_E)^2$ where P_E is pump beam power density (J/cm^2 /pulse) at the metal/prism interface, I_P is probe beam intensity (J/pulse), and R_P and R_E are probe and pump beam reflectivities, respectively. This is because S_{TRG} linearly depends both on the square of the deposited energy density of the pump light $P_E(1-R_E)$ and on the reflected light intensity of the probe beam $I_P R_P$. Here we assume that the diameter of the probe beam is smaller than that of the pump beams. Although the dependence of S_{TRG} on $I_P {P_E}^2$ has been verified for a variety of samples, incident angle-dependent behavior of S_{TRG} has not been examined. Angle changes have a large influence on S_{TRG} under SPR conditions because reflectivities are quite different, depending on the incident angle. When pump light excites the SP, we can predict S_{TRG} becomes larger for the small R_E because it is proportional to $(1-R_E)^2$. However, under SPR of the probe beam, the above simple consideration is not appropriate for the prediction of S_{TRG} on the grounds stated in the following section.[19]

B. Reflection Fresnel coefficients and SP excitation

To model this system, we start from the Fresnel theory of reflection. As is well known, no light propagating in vacuum can directly excite SP on a flat surface because light wave vector **k** for a certain energy photon is always smaller than that of SP. However, when light is incident from the dielectric medium of high refractive index *n*, SP excitation occurs at a certain incident angle because **k** could be *n* times larger in the medium. For SP excitation, we adopted the Kretschmann configuration,[20] which is a three-layer system consisting of a dielectric medium, a thin metal film of thickness *d* and a second dielectric medium, which is air in this case. Light is incident from the first dielectric medium with an incident angle of θ. SP excitation is confirmed when we measure reflectivity *R* as a function of θ, because $R(\theta)$ is the minimum at the SPR angle. The Fresnel theory predicts $R(\theta)$ as follows:

$$R = \mathbf{r}\cdot\mathbf{r}^*, \tag{1}$$

$$r(\varepsilon_2) = \frac{r_{12} + r_{23}\exp(i2k_2 d)}{1 + r_{12} r_{23}\exp(i2k_2 d)}, \tag{2}$$

$$r_{ij} = \frac{\varepsilon_i k_j - \varepsilon_j k_i}{\varepsilon_i k_j + \varepsilon_j k_i} \quad (ij = 12,23), \tag{3}$$

$$k_i = k(\varepsilon_i - \varepsilon_1 \sin^2\theta)^{1/2} \quad (i = 1,2,3), \tag{4}$$

where r is the reflection Fresnel coefficients for the three-layer structure, ε_i is the dielectric constant, k_i is the wavevector component of the electromagnetic field perpendicular to the interface and r_{ij} is the reflection Fresnel coefficient at each interface, with the subscripts i,j corresponding to each layer.

C. Modified TRG theory taking into account spatial modulation of reflection Fresnel coefficients

Like the reflectivity, the TRG signal shows the incident angle dependence. Generally, we can classify reflecting gratings into two types: amplitude grating and phase grating. A spatially periodic modulation of surface displacement, caused by SAW and thermal deformation, works as a phase grating, which is generally recognized to dominate the TRG signal generation.[21] However, under an SPR condition where the probe reflectivity approaches zero, we should consider an additional component since the small reflectivity change induced by photogenerated heat can work as an efficient amplitude grating. Thus, TRG signal intensity S_{TRG} is expressed by

$$S_{\mathrm{TRG}} = A_1(\Delta u)^2 + A_2 \cdot D_1(r_0, r_1) \tag{5}$$

as a first approximation, where Δu is the amplitude of the surface displacement normal to the surface, A_1 and A_2 are constants depending on experimental conditions, and D_1 represents diffraction efficiency expressed as a function of r_0, r_1, reflection Fresnel coefficients of the probe beam at the pump interference maxima and minima, respectively. The first term expresses spatial phase modulation as a result of surface displacement, which is detected under usual TRG experimental conditions. The second term represents light

intensity diffracted by spatial distribution of the reflection Fresnel coefficients for the three-layer structure. It is due to spatial modulation of a complex reflectivity coefficient as a result of the photoinduced change in physical properties, for which we concentrate on temperature rise in this case. As shown in the next section, the second term becomes much larger around the SPR angle.

In the transient grating theory,[22] light amplitude d_1 diffracted to the first reflecting diffraction spot is given by

$$d_1=\left(\frac{B_I}{\Lambda}\right)\int_0^{\Lambda} r(x)\exp\left(\frac{i2\pi x}{\Lambda}\right)dx, \tag{6}$$

where B_I is the amplitude of the incident beam, Λ is the grating spacing, and $r(x)$ is the amplitude of the reflection along the x direction, which is defined parallel to the grating vector. For the prism/gold/air layer structure, $r(x)$ should be replaced by the reflection Fresnel coefficients. Defining ρ_0, ρ_1, ϕ_0, ϕ_1 as the Fresnel amplitude and phase at the strengthened and weakened positions in the grating fringes, respectively, we obtain

$$r(x)=\left[\left(\frac{\rho_0+\rho_1}{2}\right)+\left(\frac{\rho_0-\rho_1}{2}\right)\cos\left(\frac{2\pi x}{\Lambda}\right)\right] \times\exp\left[i\left(\frac{\phi_0+\phi_1}{2}\right)+\left(\frac{\phi_0-\phi_1}{2}\right)\cos\left(\frac{2\pi x}{\Lambda}\right)\right]. \tag{7}$$

The Fresnel amplitude and phase are changed by temperature rise via changes in the complex refractive index $\tilde{n}=n+ik$ of the metal film. Therefore,

$$\rho_1=\rho_0+\Delta\rho(\Delta n,\Delta k)=\rho_0+\left(\frac{\partial\rho}{\partial n}\Delta n(\Delta T)+\frac{\partial\rho}{\partial k}\Delta k(\Delta T)\right), \tag{8}$$

$$\phi_1=\phi_0+\Delta\phi(\Delta n,\Delta k) =\phi_0+\left(\frac{\partial\phi}{\partial n}\Delta n(\Delta T)+\frac{\partial\phi}{\partial k}\Delta k(\Delta T)\right), \tag{9}$$

where ΔT, Δn, and Δk are the difference between the pump interference maxima and minima, of temperature, n and k, respectively. ρ_0 and ϕ_0 are the amplitude and phase of the reflection Fresnel coefficient at the ambient temperature without temperature jump and they are calculated with Eq. (2). We find by numerical evaluation that all derivatives of ρ and ϕ with respect to either n or k can be treated as constants for changes in n and k under the present experimental conditions. Δn and Δk are functions of ΔT and are calculated by the method in Sec. III D. When we predict the maximum of a transient, ΔT is regarded as temperature jump at the optical interference maxima just after the pump irradiation. We call this value $\Delta T_{\max}$ in the following. It is calculated by dividing the absorbed energy of two pump beams $2I_E(1-R_E)$ by the heat capacity of gold, where heat diffusion is neglected.

With Eqs. (6) to (9), we can evaluate D_1 as

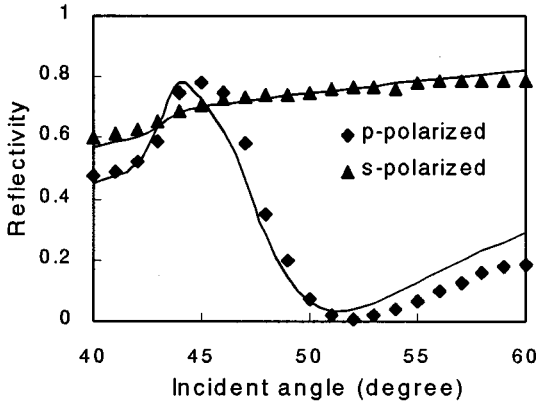

FIG. 3. The reflectivity of *p*-polarized and *s*-polarized light for the prism/gold/air structure vs incident angle. The film thickness is 36 nm. The light is incident from the prism side. The best fitted curves of reflectivity obtained by Fresnel theory are also shown.

$$D_1\propto d_1 d_1^*, \tag{10}$$

where d_1^* is the complex conjugate of d_1. Angle dependence of D_1 is compared from an experiment in Sec. IV.

D. Method for estimation of optical properties

We evaluate Δn and Δk with a method reported in the literature[23] and is summarized as follows. The Drude theory provides a good approximation for calculating the optical properties of some meals when band transition is not important. The optical constants are determined by three quantities, namely, ω_p the plasma frequency of the metal, ω the optical frequency, and ω_c the electron-phonon collision frequency, which is the reciprocal of the relaxation time of the electrons. Temperature dependence of the optical properties is dominated by the last term. The complex dielectric constant $\tilde{\varepsilon}$ is related to

$$\tilde{\varepsilon}=\tilde{n}^2, \tag{11}$$

and is expressed as

$$\tilde{\varepsilon}=1-\frac{\omega_p^2}{\omega^2+\omega_c^2}-i\frac{\omega_p^2\omega_c}{(\omega^2+\omega_c^2)\omega}, \tag{12}$$

where ω_c is a function of absolute temperature T as

$$\omega_c(T)=Kx^5\int_0^x\frac{z^4}{e^z-1}\,dz, \quad x=\frac{T_D}{T}. \tag{13}$$

Here T_D is Debye temperature and K is a constant that is actually obtained with a known ω_c value at a certain temperature.

Since the interband transition of gold mainly starts from 2.5 eV,[24] it can be ignored under our pump and probe conditions with 2.3 eV photon energy. Using Eqs. (11)–(13), we can evaluate the temperature derivatives of n and k. As their integrals over temperature rise, Δn and Δk are obtained.

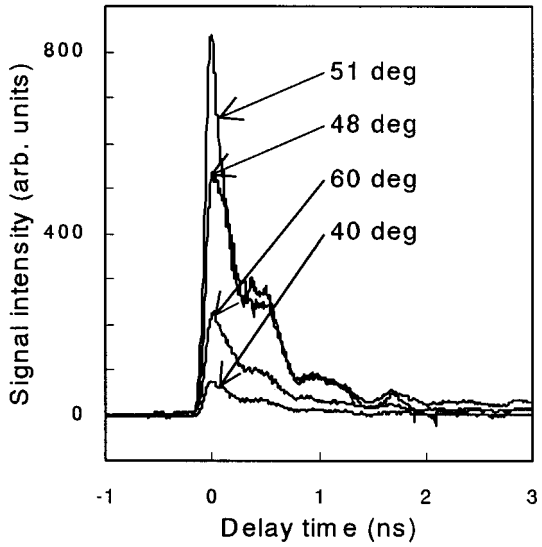

FIG. 4. Transient reflecting grating responses for the prism/gold (36 nm)/air structure at different incident angles of the laser beams. The pump beams are *p* polarized and the probe beam is *s* polarized. The fringe spacing is 1.7 μm.

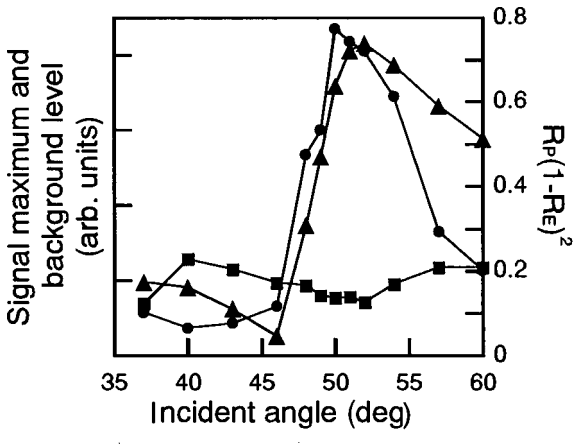

FIG. 5. Transient reflecting grating signal intensity (●); background level (■); and theoretical predicted value (▲), $R_P(1-R_E)^2$, where R_P and R_E are reflectivities of pump and probe beams, respectively, at various incident angles from 37 to 60°. The pump beams are *p* polarized and the probe beam is *s* polarized. The surface plasmon resonance angle is 51°. The experimental values are height adjusted to the theoretical predicted values.

IV. RESULTS AND DISCUSSION

A. Reflectivity curve

Angle dependence of reflectivity for the sample is shown in Fig. 3, both for *p*-polarized and *s*-polarized incident light. Reduction of reflectivity for *p*-polarized light is due to SP excitation. The SP angle is 51° and it is not in good agreement with the theoretical value, 49°, evaluated as the minimum of reflectivity calculated with Eqs. (1) to (4), where we use literature values for wavelength 539 nm as $\tilde{\varepsilon}=-6.29+2.04i$ corresponding to $\tilde{n}=0.402+2.54i$.[25] Since metal films made under different conditions often have different $\tilde{\varepsilon}$ due to the difference in defect density, concentration of contaminants and surface roughness, we carry out curve fitting for the reflectivity curve of the *p*-polarized light with the complex dielectric constant as a parameter. We obtain $\tilde{n}=0.40+2.1i$ as the best fitted value for the film thickness of 36 nm. Smooth curves in Fig. 2 are calculated with this $\tilde{n}$ both for *p*-polarized and *s*-polarized light. Experimental values are well expressed by the calculation, although a slight systematical difference still exists. We use the obtained $\tilde{n}$ later in Sec. IV C where we evaluate TRG signal enhancement under SPR with the probe beam.

B. TRG signal enhancement under SPR with the pump beams and non-SPR with the probe beam

If the two pump beams are *p* polarized and the probe beam is *s* polarized in angle-dependent TRG signal measurements, we can expect strong signal enhancement due to SPR with the pump beams as was stated in Sec. III A. Since reflectivity of the pump beams approaches zero at the SP angle as shown in Fig. 2, SP is efficiently excited by the pump beams and, almost all of the light energy is converted into heat through the nonradiative relaxation of SP. Under SPR with the pump beams, a larger amount of heat deposited to the metal film causes a larger amplitude acoustic and thermal displacement to make the TRG signal larger than for non-SPR conditions.

Angle dependence of TRG signal transients is shown in Fig. 4. For such transients, we subtract their background signal to make better comparisons for signal wave forms. Expectedly, the TRG signal intensity is 11 times larger under SPR with the pump beams (incident angle of 51°) than under the non-SPR condition of 40° incident angle. Each of the detected signal wave forms has a similar shape, composed of an exponentially decaying component along with an oscillating decay component containing information on the SAW.

Furthermore, we find the background signal level decreases around the SP angle. Figure 5 shows the signal maxima and the background signal levels at various incident angles. We predict enhancement of the signal quantitatively using conventional TRG theory as discussed in Sec. III A. In this case, I_P and P_E are constant, and then S_{TRG} is proportional to $R_P(1-R_E)^2$. These values are also plotted in Fig. 5. The experimental values are height adjusted to the theoretical predicted values. Both of them have almost the same tendency, except for angles larger than the SP angle. The difference may be caused by reduction of light power at the focused spot and alignment discrepancy of the incident beams because rotation of the sample could have some systematical influence on the light intensity per unit area as well as on the position of the focused spot.

The background in the TRG experiment comes from two components. One is the electrical background that is constant and has no influence on the experiment. The other is caused by scattered light from the solid surface. Since almost all of the light energy is absorbed at the gold surface under SPR with the pump beams, scattered light is weakened causing the background to decrease. Therefore, the signal intensity is larger while the background level is smaller as the incident angle gets closer to the SP angle.

As previously reported,[19,26] the period of the oscillation, 1.7 ns, in Fig. 4 is consistent with that calculated from SAW

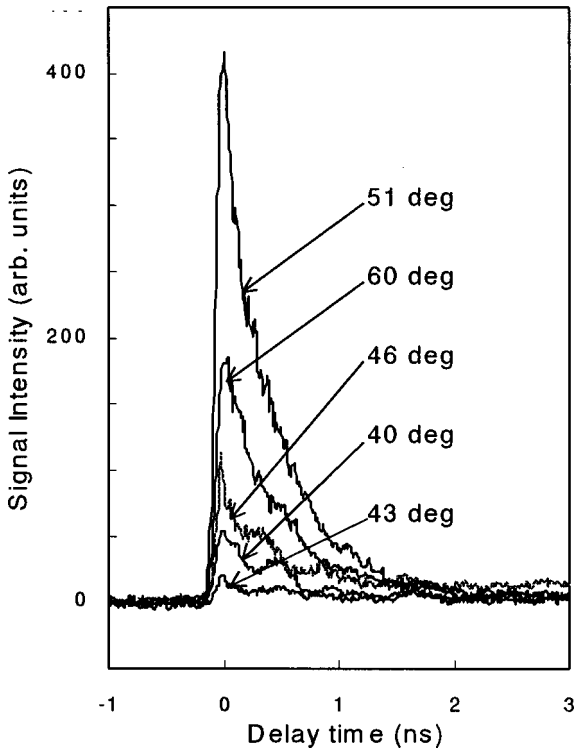

FIG. 6. Transient reflecting grating responses for the prism/gold (36 nm)/air structure at different incident angles of the laser beams. The pump beams are *s* polarized and the probe beam is *p* polarized. The fringe spacing is 1.7 μm.

velocity 2.8 km/s and grating spacing 1.7 μm. The signal enhancement and the background level suppression enables us to apply this SPR with the pump beams more easily to generate and detect GHz ultrasonics with a tunable wavelength.[26]

C. TRG signal enhancement under non-SPR with the pump beams and SPR with the probe beam

Following the simple consideration described in Sec. III A, the TRG signal amplitude S_{TRG} should decrease to zero when reflectivity R_P of the probe beam approaches zero near the SP angle because S_{TRG} is assumed to be proportional to R_P. If the two pump beams are *s* polarized and the probe beam is *p* polarized, we can expect strong signal suppression due to SPR with the probe beam at the SP angle. However, what we actually observed under SPR with the probe beam is signal enhancement accompanied by transient wave form change. When the probe beam excites SP, the TRG signal intensity is 11 times larger than under non-SPR conditions.

Angle dependence of TRG signal transients is shown in Fig. 6. The enhancement and wave form change are clearly observed. At smaller angles than 46°, the wave forms are made up of an exponentially decaying component along with an oscillating decay component. Each wave form has a similar shape to the corresponding wave form in Fig. 4. However, the wave form at 51° shows only an exponential decay. The wave form at 60° has mainly exponential decay containing a small oscillation. As we mentioned above, this wave form change cannot be explained by conventional TRG theory.

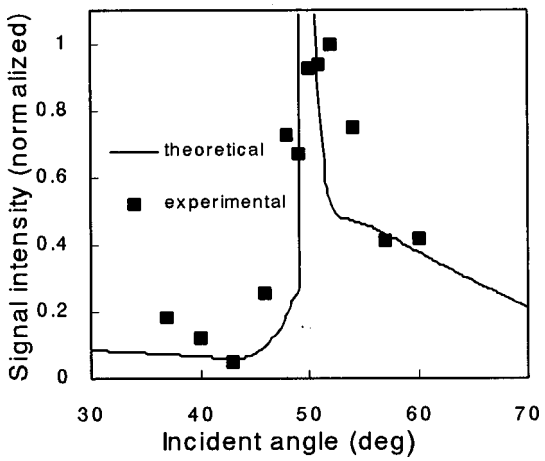

FIG. 7. Calculated intensity and maxima of the transient reflecting grating signal at the various incident angles when the probe beam is *p* polarized and the pump beams are *s* polarized. The experimental values are normalized by the signal at 52°, which is the largest value in the range from 37° to 60°. Amplitude of the theoretical values are height adjusted to the experimental data in order to make comparison easier.

We introduced a component to modify the TRG theory in Sec. III C. The second term in Eq. (5) expresses diffraction caused by a spatial change in the reflecting Fresnel coefficients coming from change in refractive and extinction indexes. Why this component enhances the TRG signal under SPR with the probe beam is qualitatively explained as resulting from the SPR condition being very sensitive to changes in optical properties of the metal film. When the temperature distribution causes spatial modulation of the refractive index, efficiency of SP excitation is critically position-dependent for a probe beam incident around the SPR angle. The resultant nonuniform absorption of the probe beam causes reflecting diffraction to increase. It is easy to explain the observed wave form change if the theory predicts strong signal enhancement under SPR of the probe beam because the dominant term becomes different. When the $(\Delta u)^2$ term in Eq. (5) dominates, TRG signal shows an exponential decay along with an oscillation because Δu is a mixture of the relaxations of thermal and acoustic displacements. On the other hand, the TRG signal has exponential decay and no oscillation when the D_1 term dominates because the cooling process of the distributed temperature rise causes D_1, where the acoustic waves have no contribution to the TRG signal.

The remaining problem is whether the theory predicts sufficient enhancement. We calculated D_1 to examine the enhancement. The calculation was carried out using the complex refractive index of this sample obtained in Sec. IV A and as explained in Sec. III C.

In our experiment, Δn and Δk were calculated as 0.035 and -0.018, respectively, for estimated ΔT_{max} of 50 K. We calculated D_1 at different incident angles and we evaluated signal intensity by neglecting the surface displacement term. Figure 7 shows the calculated signal intensity and experimental results of TRG signal maxima. The experimental data

are normalized to a unit intensity with the largest value observed at 52°, while amplitude of the theoretical values are height adjusted to the experimental data in order to make comparison easier. As shown in Fig. 7, the theory predicts substantial signal enhancement around and above the SP angle. From this result we confirm that the mechanism of signal enhancement under SPR with the probe beam is due to spatial modulation of the reflection Fresnel coefficients.

Quantitatively, there are some problems with the theory. The theory predicts the TRG signal intensity diversely increases just around the SP angle, but we could not observe such a sharp peak experimentally. As shown in Fig. 7, by adjusting relative intensities, we can plot the experimental data and the theoretical curves in a manner that they have the same tendency, except just around the sharp peak at the SP angle. The peak center is at 49.2° and the full width at half maximum is 1.0°. We can give some possible reasons. The peak width is so small that we may have accidentally skipped the appropriate angle range for the stronger enhancement in the present experiment, scanning the incident angle step by step where the minimum step width was 1°. Another reason is that the theoretical values in Fig. 7 depend critically on Δn and Δk values. These values were evaluated with the interband transitions considered to be negligible. There are interband transitions from the *d* band to the Fermi surface of their starting energy of 1.9 eV, but this treatment seems appropriate because they are reported to have less influence on the optical constants than electrons, expressed by the Drude theory, around the wavelength 532 nm used in this experiment.[27,28] Further improvement of the angle resolution is required to clarify these points.

Another problem with the theory is as follows. If we note the measured signals for lower angles, the observed intensity takes a minimum at 43° and intensities at 46° and 40° are 6 and 3 times larger than the minimum, respectively. The theory also predicts a minimum in the signal intensity at 43.7°, but the intensity does not increase so much at lower angles. The difference between the experimental and theoretical behaviors is caused by omission of the $(\Delta u)^2$ component in this calculation. As shown in Fig. 6, these wave forms contain oscillation by SAW. Then we must consider the $(\Delta u)^2$ component too, in order to interpret them. As noted in the following paragraph, intensities of the mixed signal of $(\Delta u)^2$ and D_1 components cannot be easily explained.

Comparing the three wave forms for 40°, 43°, and 46° in Fig. 6, we see that the wave form at 46° has a different oscillation phase than the others. We should recall that reflectivity of *p*-polarized light had a maximum at 45° as shown in Fig. 3. That angle is the critical angle of the attenuated total reflection. Above that angle, the interface-normal component of the light wave vector in air is converted from a real number to an imaginary one. The spatial distribution of the electromagnetic field inside and near the gold film has a dramatic change at the critical angle. In Eq. (5), we assumed a simple superposition between $(\Delta u)^2$ and D_1. This treatment is valid only for some limited cases such as when one of them dominates the TRG signal. Generally, phase change at reflection can interfere with that of displacement. We can explain wave form behaviors near the total reflection angle by taking this interference in phase into account. When the difference of the deposited heat quantity at each angle is neglected, roughly speaking, light diffracted by SAW keeps its phase during the angle change while that by spatial distribution of the reflection Fresnel coefficients can change its phase, then the timing of the destructive or constructive interference has a 180° phase change. Observed results in Fig. 6 support the conclusion that the spatial distribution of the reflection Fresnel coefficients has substantial influence on the TRG signal.

From an experimental viewpoint, we can expect to detect signals mainly due to SAW at a smaller angle than the SP angle, which deduces the elastic properties. Thermal characteristics can be separately deduced from TRG signals observed around the SP angle. It has been difficult to analyze the TRG signal which is a complicated mix of thermal and acoustic signals, but with these measurements, we can estimate the ratio of thermal and acoustic contributions for any TRG signal at a given incident angle. The angle dependence measurement using the *p*-polarized probe beam will enable us to separate the components of the TRG signal and it will provide more exact analysis of the characteristic physical properties of the metal film and a second dielectric medium. Then the theory presented here sufficiently explains the TRG signal enhancement accompanying wave form change qualitatively, although it contains some points for further quantitative discussion.

D. TRG signal enhancement under SPR with the pump and probe beams

SP excitation by either *p*-polarized pump or probe beams enhances the TRG signal. Here we examine the TRG signal when both pump and probe beams are *p* polarized. We reduced the intensity of the pump beams and the probe beam to 30% and 20%, respectively, with respect to the experimental conditions presented above. The expected TRG signal intensity is reduced to 1.8% compared with the usual condition, according to the theory in Sec. III. It should be noted that self-diffraction caused by interference between one of the pump beams and the probe beam is not detected in the present experimental setup because diffraction spots by self-diffraction are spatially separated from the spot we used to detect the signal.

Under SPR with the pump and probe beams, the physical origin of signal enhancement is expected as follows. At first an enhanced TRG is gotten because of the high conversion efficiency from light to heat using the SPR with the pump beams and then the TRG is detected at high sensitivity with the SPR with the probe beam, where the thermal component is selectively enhanced. Transient wave forms measured at three incident angles are shown in Fig. 8. Each of them differs from the signals presented so far and has a sharp peak, whose width is approximately equal to that of the optical pulse duration, followed by an exponential decay like that typically observed for the SPR with the probe beam. Both the sharp peak and the following component have a maximum intensity at the SP angle incidence and their intensities decrease for angles other than the SP angles. This signal is not detected for smaller angles than 45°.

By replacing the optical wave guide for detecting light on one of the self-diffraction spots, we observed autocorrelation of the optical pulse. The result is shown in Fig. 9 with one of

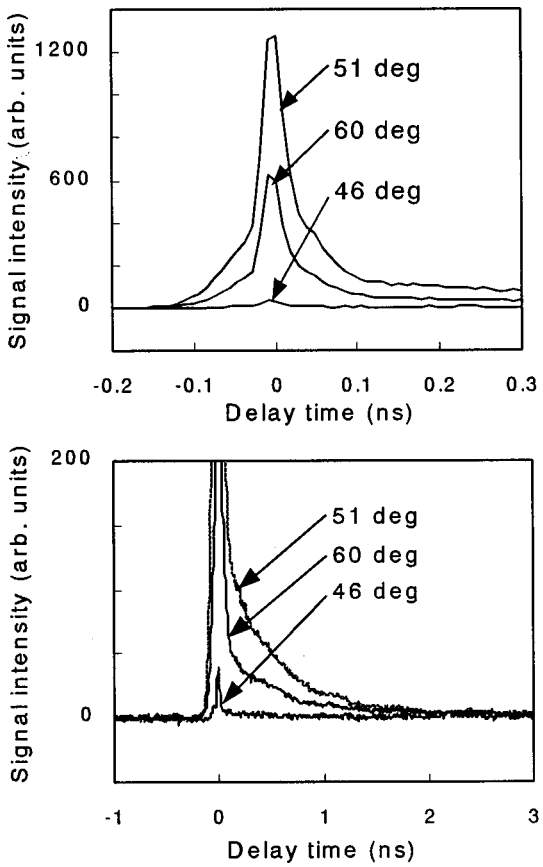

FIG. 8. Transient reflecting grating responses for the prism/gold (36 nm)/air structure at different incident angles of laser beams. Both the pump beams and the probe beam are *p* polarized. The upper and lower graphs show the transient wave forms at 0.3 and 3 ns, respectively. The former and latter show the first peak and the exponential decay following it, respectively. The signal intensity value of the former corresponds to that of the latter.

the TRG signal transients measured under the same experimental conditions except for the waveguide setting at an appropriate position. Both traces are intensity normalized to unity. They have different responses and the TRG signal shows some relaxation. Assuming the signal is made up of some exponential decays convoluted with the incident pulse, we carried out fitting of the experimental wave form. The faster one of the two relaxation times of the signal is determined as 10 ± 5 ps.

When we consider its physical meaning, electrons in nonthermal equilibrium seem essential. Photoexcited electrons, which are not SP itself, are one possible cause of the phenomena we observed although they are known to relax in gold through electron-phonon coupling within a few picoseconds.[29] So they seem to have too fast a relaxation time. Based on the fact that this signal is detected only around the SP angle and it clearly shows a larger intensity change than the heat relaxation component, we think this signal is caused by the excited electrons made through the relaxation of SP. The 10 ps relaxation time observed could be caused by a longer mean free path for the excited electrons induced by SP than that for the normally excited electrons. We have no clear explanation why the signal was enhanced by such electrons. The electrons generated through

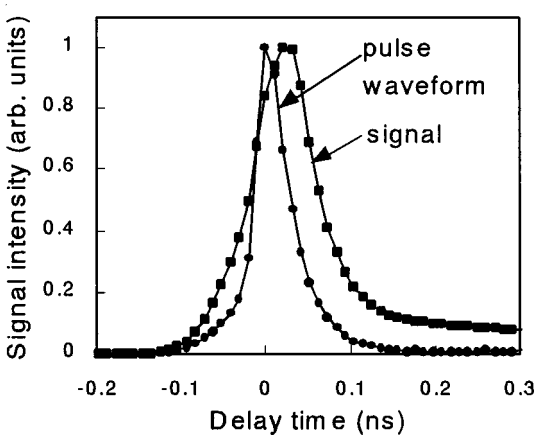

FIG. 9. First peak of the transient reflecting grating signal when both pump beams and the probe beam excite surface plasmon. The autocorrelation trace of the optical pulse is also shown. Time 0 is adjusted to the time when the autocorrelation trace takes a maximum.

the collective oscillation of electrons, namely SP, might change the optical properties more dramatically than those generated by the simple optical excitation. Measurements with high time resolution should clarify this and we are now making them. Anyway we have detected some dynamic behavior of the excited electrons, with almost 100 times larger intensity, using this configuration, which will be more effective for the measurement of electronic interactions in metals for time scales much shorter than tens of picoseconds.

V. CONCLUSION

We developed a TRG method under three types of SPR conditions of two pump beams, one probe beam only, and two pump beams and a probe beam. Each of them gave enhancement in the TRG signal.

When the pump beams excited the SP, the TRG signal was enhanced quadratically in proportion to the absorbed energy amount of the pump beams due to the high efficiency from light to heat via SP. The SPR with the pump beams provide good signal intensity and low background and enabled us to detect GHz ultrasonics easily.

Under the SPR with the probe beam, the TRG signal was also enhanced but this enhancement involved a signal wave form change. This signal originated from the spatial reflection Fresnel coefficient change caused by the temperature rise. This component would be a secondary component under usual conditions, but it became so large around the SP angle that it dominated the signal. Our modified TRG theory qualitatively explained this phenomenon. TRG signals were usually observed as a mix of components affected by heat and SAW relaxation. The enhancement of the pure thermal term will enable us to separately detect each component.

Under the SPR with the pump beams and the probe beam, we detected a component representing dynamics of electrons probably in nonthermal equilibrium and related to SP. This result may provide a physical insight into SP. This signal was much larger than any other components, which promises that this method is preferable for the detection of ultrafast

electronic interactions in metals.

Each of the three SPR conditions will have application fields of TRG, especially for research on various electronic, thermal and acoustic interactions in thin films and at interfaces of metal-liquid, metal/adsorbate, and so on. Advantages of TRG, combined with the excellent sensitivity of SP for interfaces, will lead to acquisition of unique information on nanometer-scale properties.

[1] R. K. Chang and T. E. Furtak, *Surface Enhanced Raman Scattering* (Plenum, New York, 1982).

[2] H. J. Simon, D. E. Mitchell, and J. G. Watson, Phys. Rev. Lett. **33**, 1531 (1974).

[3] A. Lookene, R. Savonen, and G. Olivecrona, Biochemistry **36**, 5627 (1997).

[4] C. E. Jordan and R. M. Corn, Anal. Chem. **69**, 1449 (1997).

[5] W. Wang, M. J. Feldstein, and N. F. Scherer, Chem. Phys. Lett. **262**, 573 (1996).

[6] M. Exter and A. Lagendijk, Phys. Rev. Lett. **60**, 49 (1988).

[7] R. V. Andaloro, H. J. Simon, and R. T. Deck, Appl. Opt. **33**, 6340 (1994).

[8] M. Prochazka, P. Mojzes, B. Vlckova, and P. Turpin, J. Phys. Chem. B **101**, 3161 (1997).

[9] K. A. O'Donnell, R. Torre, and C. S. West, Phys. Rev. B **55**, 7985 (1996).

[10] X. Sun, S. Shiokawa, and Y. Matsui, J. Appl. Phys. **69**, 362 (1991).

[11] S. I. Bozhevolnyi, I. I. Smolyaninov, and A. V. Zayats, Phys. Rev. B **51**, 17 916 (1995).

[12] X. Chen, K. M. Shakesteff, M. C. Davies, J. Heller, C. J. Roberts, S. J. B. Tendler, and P. M. Williams, J. Phys. Chem. **99**, 11 537 (1995).

[13] A. Harata, T. Edo, and T. Sawada, Chem. Phys. Lett. **249**, 112 (1996).

[14] A. Harata, T. Kawasaki, M. Ito, and T. Sawada, Anal. Chim. Acta **299**, 349 (1995).

[15] T. Tanaka, A. Harata, and T. Sawada, Jpn. J. Appl. Phys., Part 1 **35**, 3642 (1996).

[16] A. Harata and T. Sawada, Trends Anal. Chem. **14**, 504 (1995).

[17] T. Sawada and A. Harata, Appl. Phys. A: Mater. Sci. Process. **61A**, 263 (1995).

[18] Q. Shen, A. Harata, and T. Sawada, J. Appl. Phys. **77**, 1488 (1995).

[19] K. Katayama, Q. Shen, A. Harata, and T. Sawada, Appl. Phys. Lett. **69**, 2468 (1996).

[20] E. Kretschmann, Z. Phys. **241**, 313 (1971).

[21] A. Harata, Q. Shen, T. Tanaka, and T. Sawada, Jpn. J. Appl. Phys., Part 1 **32**, 3633 (1993).

[22] H. J. Eichler, P. Gunter, and D. W. Pohl, *Laser-Induced Dynamic Gratings* (Springer-Verlag, Berlin, 1986), pp. 94–99.

[23] K. Ujihira, J. Appl. Phys. **43**, 2376 (1972).

[24] D. E. Aspnes, E. Kinsbron, and D. D. Bacon, Phys. Rev. B **21**, 3290 (1980).

[25] D. W. Lynch and W. R. Hunter, *Handbook of Optical Constants of Solids* (Academic, Boston, MA, 1991), p. 286.

[26] K. Katayama, Q. Shen, A. Harata, and T. Sawada, in *Proceedings of the Acoustical Society of America and Acoustical Society of Japan, Third Joint Meeting*, Honolulu, 1996, edited by S. Kumano (Osaka University, Tokyo, 1996), p. 575.

[27] P. Winsenius, M. Guerrisi, and R. Rosei, Phys. Rev. B **12**, 4570 (1975).

[28] M. Guerrisi, R. Rosei, and P. Winsemius, Phys. Rev. B **12**, 557 (1975).

[29] R. W. Schoenlein, W. Z. Lin, J. G. Fujimoto, and G. L. Eesley, Phys. Rev. Lett. **58**, 1680 (1987).